

# Effects of *Lyrm1* knockdown on mitochondrial function in 3 T3-L1 murine adipocytes

Guan-Zhong Zhu · Min Zhang · Chun-Zhao Kou ·  
Yu-Hui Ni · Chen-Bo Ji · Xin-Guo Cao · Xi-Rong Guo

Received: 7 August 2011 / Accepted: 9 November 2011 / Published online: 15 January 2012  
© Springer Science+Business Media, LLC 2012

**Abstract** To explore the effects of *Lyrm1* knockdown on the mitochondrial function of 3 T3-L1 adipocytes using small interfering RNA (siRNA). 3 T3-L1 preadipocytes were infected with either a negative control (NC) expression lentivirus or a *Lyrm1*-shRNA expression lentivirus and induced to differentiate. The knockdown efficiency of *Lyrm1*-specific shRNA in 3 T3-L1 cells was evaluated by real-time PCR. The ultrastructure of the mitochondria in adipocytes was visualized using transmission electron microscopy after differentiation. The levels of mitochondrial DNA copy numbers and *Ucp2* mRNA were detected by real-time quantitative PCR. The levels of ATP production was detected using a photon-counting luminometer. The mitochondrial membrane potential and ROS levels of cells were analyzed with a FACScan flow cytometer using Cell Quest software. Cells transfected with lentiviral-*Lyrm1*-shRNA showed a significantly reduced transcription of *Lyrm1* mRNA compared with NC cells. The size and ultrastructure of mitochondria in *Lyrm1* knockdown adipocytes was similar to those of the NC cells. There was no significant difference in mtDNA copy number between the two groups. The total level of ATP production, mitochondrial membrane potential

and *Ucp2* mRNA expression levels were dramatically increased in adipocytes transfected with *Lyrm1* RNAi. Furthermore, the level of ROS was dramatically decreased in *Lyrm1* knockdown adipocytes. Knockdown of the *Lyrm1* gene in adipocytes resulted in dramatically increased cellular ATP production, mitochondrial membrane potentials and levels *Ucp2* mRNA, while ROS levels were significantly decreased. These results imply that mitochondrial function is improved in adipocytes after the knockdown of *Lyrm1*.

**Keywords** Obesity · RNA interference · Mitochondria · *Ucp2*

## Abbreviations

LYRM1	Homo sapiens LYR motif containing 1
ROS	reactive oxygen species
UCP2	uncoupling protein 2
siRNA	small interfering RNA
shRNA	short hairpin RNA
mRNA	messenger ribonucleic acid
mtDNA	mitochondrial DNA
IR	insulin resistance
NC	negative control
cDNA	single-stranded complementary DNA

Guan-zhong Zhu and Min Zhang contributed equally to this work

G.-Z. Zhu · C.-Z. Kou · C.-B. Ji  
Institute of Pediatrics, Nanjing Medical University,  
Nanjing 210029, China

M. Zhang · Y.-H. Ni · X.-G. Cao (✉) · X.-R. Guo (✉)  
Nanjing Maternal and Child Health Care Hospital of Nanjing  
Medical University,  
No.123 Tianfei Lane,  
Nanjing 210004, China  
e-mail: xgcao@njmu.edu.cn  
e-mail: xrguo@njmu.edu.cn

## Introduction

Obesity has become an important global public health problem in recent decades (Jeffery and Sherwood 2008). It has reached epidemic proportions worldwide and is associated with severe metabolic and cardiovascular complications (Kopelman 2000; Spiegelman and Flier 2001; Visscher

and Seidell 2001). Common obesity results from interactions between genetic, environmental, and psychosocial factors (Walley et al. 2009). An important consequence of obesity is the development of insulin resistance (IR), which is considered to be an important link between adipocytes and the associated risks of type 2 diabetes and cardiovascular disease (Ferrannini et al. 2007; Qatanani and Lazar 2007; Reaven 1997). IR is defined as a condition in which normal insulin concentrations fail to produce normal glucose metabolism (Kahn 1978). To date, the mechanisms that underlie IR remain unclear. Genetic factors, oxidative stress, mitochondrial biogenesis, and aging may affect mitochondrial functions, leading to IR and various pathological conditions (Kim et al. 2008). Numerous studies have indicated that mitochondrial defects play a critical role in obesity-associated IR (Lowell and Shulman 2005; Maasen 2008). Evidence from one study has demonstrated that obesity/diabetes is accompanied with impaired mitochondria in the adipose tissue of db/db mice (Choo et al. 2006). A correlation between mitochondrial dysfunction in adipose tissue and obesity/diabetes in humans has also been proposed (Dahlman et al. 2006; Hammarstedt et al. 2003).

In our earlier studies, we isolated and characterized *Homosapiens* LYR motif containing 1 (*LYRM1*), a novel human gene that shows increased expression in obese subjects. The 122-amino-acid LYRM1 protein is encoded by a gene with four exons that maps to chromosome 16. Further results have shown that LYRM1 promotes preadipocyte proliferation and inhibits preadipocyte apoptosis (Qiu et al. 2007; Qiu et al. 2009). Our studies also revealed that the overexpression of LYRM1 resulted in IR in adipocytes by reducing insulin-stimulated glucose uptake, and we hypothesized that the accompanying mitochondrial dysfunction might be a potential mechanism that underlies this effect (Cao et al. 2010). Genetic factors, oxidative stress, mitochondrial biogenesis and aging may affect mitochondrial function, leading to IR and consequent pathologies (Cao et al. 2010). The aim of this present study was to interpret the effects of *Lyrm1*, the homologous protein in mice, on the mitochondrial function of 3 T3-L1 murine adipocytes by silencing its expression using small interfering RNA (siRNA).

## Materials and methods

### Cell culture and differentiation

3 T3-L1 preadipocytes were cultured in high glucose concentration Dulbecco's modified Eagle's medium (DMEM) containing 10% fetal bovine serum (FBS), and were maintained in a humidified atmosphere at 37 °C with 5% CO<sub>2</sub>. Cell differentiation into adipocytes was achieved using a previously described method (Niimi et al. 2009).

### ShRNA lentivirus preparation and plasmid construction

The expression lentiviral plasmid for short hairpin RNA (shRNA) of mouse *Lyrm1* or a negative control (NC) were constructed by inserting a fragment of DNA for shRNA expression into a pgLV-U6-puro expression vector. The recombinant vector was named pgLV-U6-puro-*Lyrm1*-shRNA or pgLV-U6-puro-NC-shRNA. The sequences of the cDNA fragment (positive-sense strand) were as follows: *Lyrm1*, 5' GCAATCATTCTAGACTAA; negative control, 5'-TTCTCCGAACGTGTCACGT.

A 19-nt short hairpin RNA (shRNA) targeting sequence was designed according to the mouse *Lyrm1* mRNA sequence in the GenBank database (NM\_029610.2). The designed shRNA construct contained a 19-nt double-stranded sequence, which was an inverted complementary repeat that formed a loop sequence (5'-CTCGAG-3'). The 5' overhangs, CCGG and AATT, were added for ligation into *Age*I- and *Eco*RI-digested pgLV-U6-puro expression vector in the positive-sense and antisense strands, respectively.

### Stable shRNA transfection of 3 T3-L1 cells by lentiviral infection

The lentiviral supernatant was produced by transient transfection of HEK-293 T cells. HEK-293 T cells were transfected with an expression lentiviral plasmid with a packing (pGag/Pol), VSV-G-expressing (pVSV-G) and a Rev (pRev)-expressing plasmid by the Chen-Okayama method (Chen and Okayama 1987). The medium containing lentiviruses was collected and filtered after 60 h of transfection. 3 T3-L1 preadipocytes were infected with this medium supplemented with 5 µg/ml polybrene for 24 h in DMEM. After cells were washed with normal medium and diluted in 6-well plates; puromycin (2.5 µg/ml) was added into culture medium for another 4 days before further experiments.

### RNA extraction and quantitative real-time PCR

Total RNAs from 3 T3-L1 cells transfected with lentiviral *Lyrm1*-shRNA or lentiviral-NC-shRNA were extracted using TRIzol reagent (Invitrogen). Reverse transcription was performed using an AMV Reverse Transcriptase kit (Promega, Madison, WI, USA) using random hexamer primers. Real-time PCR was performed using an Applied Biosystems 7300 Sequence Detection System (ABI 7300SDS; Foster City, CA, USA) according to the manufacturer's protocols. The relative mRNA level in transfectants was normalized against the mRNA levels of an endogenous control gene, *β-actin*. The sequences of the primers are shown in Table 1.

**Table 1** Sequences for primer used in real-time PCR

Gene	Forward primer (5'-3')	Reverse primer (5'-3')	Probe
CytB	TTTTATCTGCATCTGA	CCACTTCATCTTACCAT	AGCAATCGTTACCTCCCT
	GTTTAATCCTGT	TTATTATCGC	CTTCCTCCAC
28S	GGCGGCCAAGCGTTC	AGGCGTTCAGTCATAAT	TGGTAGCTTCGCCCCATT
	ATAG	CCCACAG	GGCTCCT
LYRM1	AGGGCAGATGGAA	GATGGATAGGGCGTG	
	GACACC	GATAA	
UCP4	AAGGCTTCCTAAA	GACCATCCGACCTCC	
	GCTGTGGC	AGAGT	
$\beta$ -actin	TCACCCACACTGTG	CAGCGGAACCGCTCAT	
	CCCATCTACGA	TGCCAATGG	

### Electron microscopy

On the 10th day of differentiation, the mature adipocytes were collected after trypsin digestion, washed in phosphate buffered saline (PBS; pH 7.4), and fixed in a buffer containing 2.5% glutaraldehyde and 4% paraformaldehyde. The cells were then washed in 0.1 M cacodylate buffer, post-fixed with 1% osmium tetroxide and 1.5% potassium ferrocyanide for 1 h, washed in water, stained with 1% aqueous uranyl acetate for 30 min, and dehydrated through a graded series of ethanol to 100%. The samples were then infiltrated and embedded in TAAB Epon (Marivac Canada Inc., St. Laurent, Canada). Ultra-thin sections (60 nm) were cut on a Reichert Ultracut-S microtome, placed onto copper grids, stained with uranyl acetate and lead citrate, and examined on a transmission electron microscope (JEM-1010; JEOL, Tokyo, Japan) at an accelerating voltage of 80 KV.

### Real-time PCR for mitochondrial DNA (mtDNA)

Relative amounts of mtDNA were determined by real-time qPCR, as previously described (Kaaman et al. 2007). Briefly, DNA was isolated from adipocytes with a DNA extraction kit (Baitaike, Beijing, China) and quantified by spectrophotometry at 260 nm. Two primer sets were used for PCR analysis. A 110-nt mtDNA fragment within the *Cytb* gene was used for the quantification of mtDNA. The PCR product was previously cloned into the plasmid pMD-T 18 and verified by DNA sequencing. Plasmid standards of known copy numbers were used to generate a log-linear standard curve, from which the *Cytb* copy numbers of the studied samples could be determined by real-time PCR. A 291-bp region of the nuclear gene for 28S ribosomal RNA (rRNA) was used to normalize the results. A standard curve of plasmid containing the 28S fragment was used to determine the copy numbers of the studied samples. The ratio of mtDNA to nuclear DNA reflects the concentration of

mitochondrial per cell. The sequences of the primers are shown in Table 1.

### ATP production

On the 10th day of differentiation, the ATP content of adipocytes was measured using a luciferase-based luminescence assay kit (Biyuntian, Nantong, China). Briefly, the adipocytes were homogenized in an ice-cold ATP-releasing buffer. Treated adipocytes were mixed with the detection reagent for 5 min. Light emission was recorded for 30 s using a photon-counting luminometer. The relative ATP level was normalized by protein concentration determined by the BCA method.

### Confocal laser microscopy

Mito-Tracker Red, a red mitochondria-specific cationic fluorescent dye (Molecular Probes, Invitrogen, Carlsbad, CA, USA), was used to estimate the mitochondrial membrane potential ( $\Delta\Psi_m$ ). The H2-DCFDA probe (Sigma, St. Louis, MO, USA) was used to evaluate the intracellular ROS levels (Maxwell et al. 1999). On the 10th day of differentiation, the transfected 3 T3-L1 adipocytes were incubated with 150 nM of Mito-Tracker Red and 5  $\mu$ M of H2-DCFDA for 30 min at 37 °C and then washed three times with warm PBS. Cells were imaged using a confocal laser scanning microscope (Zeiss, Gottingen, Germany).

### Flow cytometry

On the 10th day of differentiation, the 3 T3-L1 adipocytes were incubated with 150 nM MitoTracker and 5  $\mu$ M of H2-DCFDA at 37 °C. After 30 min, cultured cells were trypsinized and centrifuged at 1,000 rpm at 4 °C for 5 min, then resuspended in Krebs-Ringer solution buffered with 4-(2-hydroxyethyl)-1-piperazine ethanesulfonic acid (HEPES)

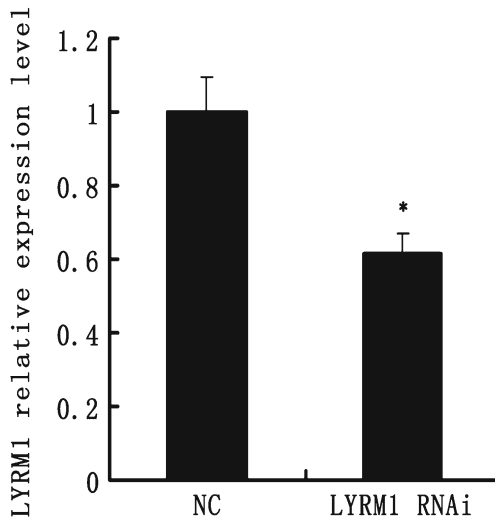


**Fig. 1** Knockdown of *Lyrm1* mRNA expression by siRNA. *Lyrm1* mRNA relative to  $\beta$ -actin in the lentiviral-*Lyrm1*-shRNA-transfected 3 T3-L1 preadipocytes was examined by real-time PCR in comparison with lentiviral-NC-shRNA-transfected 3 T3-L1 preadipocytes. The mRNA inhibitory efficiency was 39% ( $P<0.05$  vs. NC adipocytes)

and 0.5% bovine serum albumin. Cells were analyzed with a FACScan flow cytometer using Cell Quest software (BD Biosciences, San Jose, CA, USA).

#### Statistical analysis

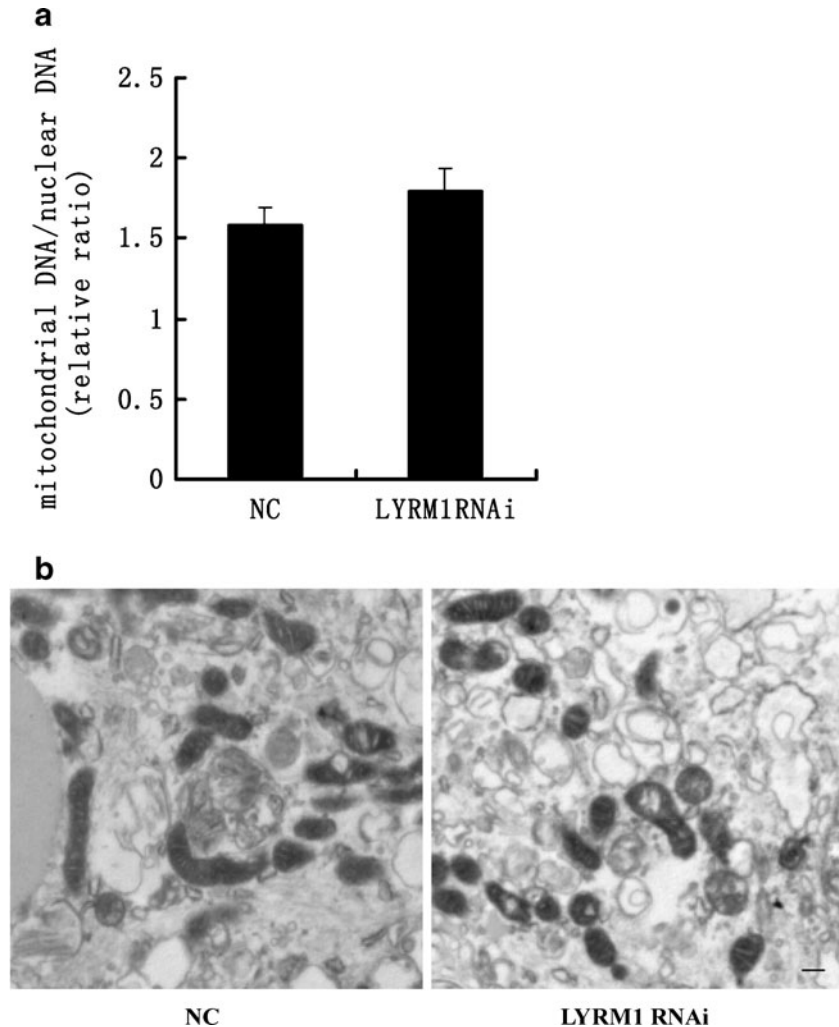
Each experiment was performed at least three times. All data are expressed as the means  $\pm$  SEM. Statistical analysis was performed using one-way ANOVA or Student's *t*-test with the SPSS 10.0 statistical software package (SPSS Inc., Chicago, IL, USA), and  $p$ -values  $<0.05$  were considered to be statistically significant.

#### Results

##### Suppression of *Lyrm1* expression by small interfering RNA

As shown in Fig. 1, cells transfected with lentiviral-*Lyrm1*-shRNA showed a significantly reduced transcription of *Lyrm1*

**Fig. 2** Effects of *Lyrm1* knockdown on the mitochondrial DNA copy number and mitochondrial morphology in 3 T3-L1 adipocytes. The negative control (NC) cells were induced to differentiate. On the 10th day of differentiation, cellular mtDNA content was detected by real-time PCR analysis with primers designed to the *Cytb* and 28S rRNA genes ( $n=6$ ). The *Cytb* to 28S rRNA gene ratio reflects the concentration of mitochondria per cell **a**. The ultrastructure of mitochondria in the adipocytes was visualized by transmission electron microscopy. The scale bar in the bottom right corner of **b** represents 1  $\mu$ m **b**



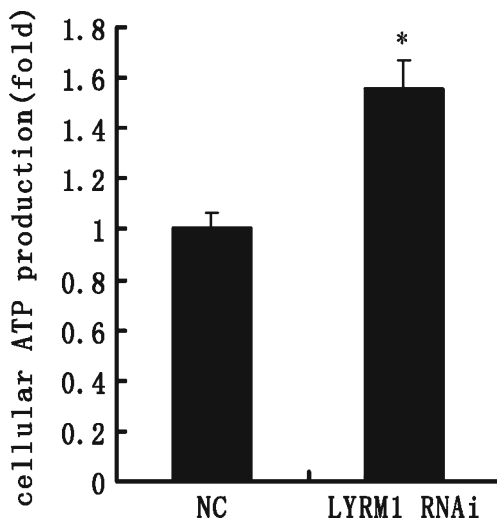


**Fig. 3** Effects of *Lyrm1* silencing on cellular ATP production. The transfected 3 T3-L1 preadipocytes were induced to differentiate. On the 10th day of differentiation, the cellular ATP production was measured and normalized to the protein concentration. \* $P<0.05$  in comparison with the NC adipocytes ( $n=6$ )

mRNA when compared with negative control (NC) cells ( $P<0.05$ ). The steady state *Lyrm1* mRNA level of the lentiviral-*Lyrm1*-shRNA-transfected cells was 61% that of the NC cells.

#### Effect of *Lyrm1* knockdown on mtDNA copy number and mitochondrial morphology

The mtDNA copy number per mitochondria is generally considered to be constant in most mammalian cell types (Robin and Wong 1988). Therefore, the mtDNA copy number is generally considered as an indicator of cellular mitochondrial number. Using real-time PCR, we assessed the effects of *Lyrm1* knockdown on mtDNA copy number, and the results showed that there was no significant difference in mtDNA copy number between the two groups in this study ( $p>0.05$ ). Mitochondrial morphology is closely related to mitochondrial function and metabolic activity (Brocard et al. 2003). Therefore, we investigated the morphology of the mitochondria using electron microscopy. As shown in Fig. 2, the morphology of mitochondrial in *Lyrm1* knockdown adipocytes was similar to that of the NC cells. The size and

**Fig. 4** Effect of *Lyrm1* knockdown on mitochondrial membrane potential. The transfected 3 T3-L1 preadipocytes were induced to differentiate. On the 10th day of differentiation, the mature adipocytes were stained with MitoTracker Red, imaged using a confocal laser scanning microscope **a**, and analyzed with a FACScan flow cytometer. \* $P<0.05$  in comparison with the NC adipocytes (**b**;  $n=6$ )

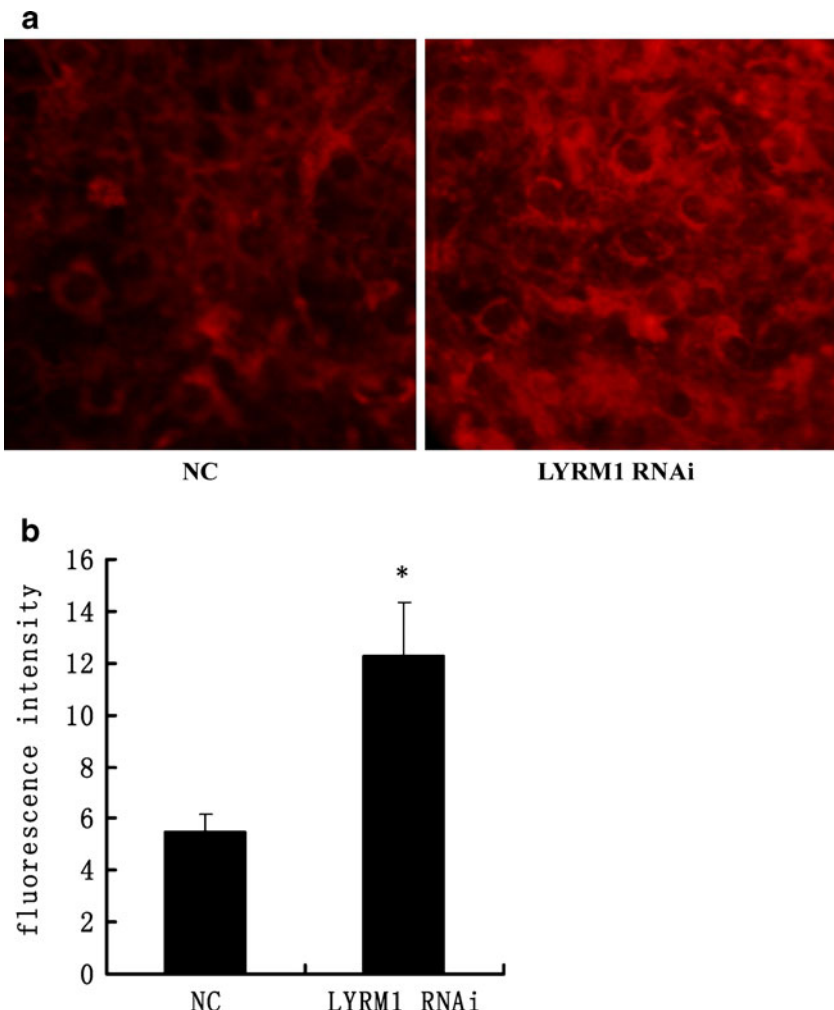
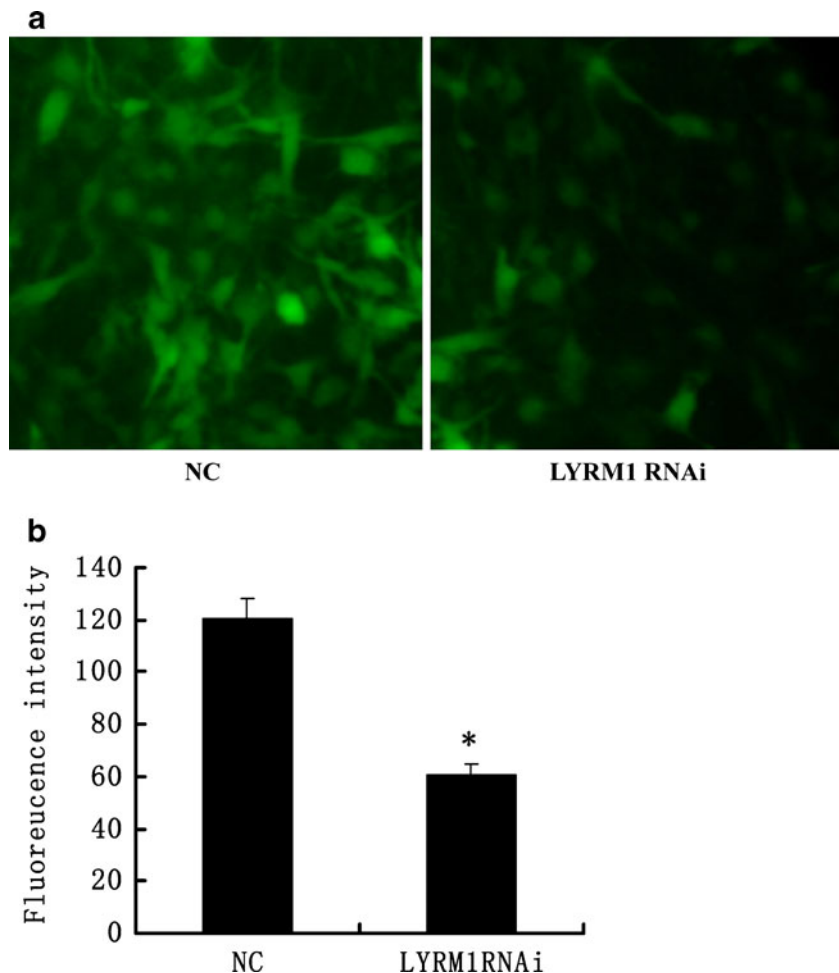


**Fig. 5** *Lyrm1* knockdown decreases cellular levels of reactive oxygen species (ROS) in adipocytes. The transfected 3 T3-L1 preadipocytes were induced to differentiate as described in the Materials and Methods. On the 10th day of differentiation, the mature adipocytes stained with the H2-DCFDA probe were imaged using a confocal laser scanning microscope **a** and the ROS levels in the adipocytes were determined using a FACScan flow cytometer. \* $P<0.05$  in comparison with the NC adipocytes (b;  $n=6$ )



ultrastructure of the mitochondria were not altered after the *Lyrm1* knockdown.

#### Effects of *Lyrm1* silencing on cellular ATP production

As shown in Fig. 3, we found that the total ATP production was dramatically increased in adipocytes transfected with *Lyrm1* RNAi.

#### Effects of *Lyrm1* knockdown on $\Delta\Psi_m$

As shown in Fig. 4a and b, the adipocytes that were subjected to *Lyrm1* interference were strongly stained with MitoTracker Red compared to the NC adipocytes. The  $\Delta\Psi_m$  was greatly increased in *Lyrm1* knockdown adipocytes compared with NC adipocytes.

#### Effects of *Lyrm1* knockdown on cellular ROS and *Ucp2* mRNA levels

As shown in Fig. 5a and b, ROS levels in the *Lyrm1*-silenced adipocytes were much lower than that in the NC adipocytes. *Lyrm1* knockdown dramatically decreased the

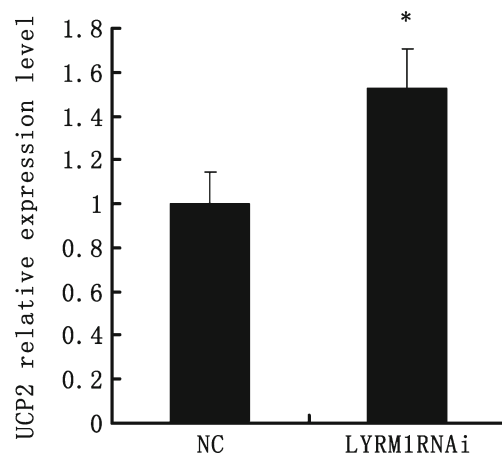


**Fig. 6** Effects of *Lyrm1* knockdown on *Ucp2* mRNA levels. *Lyrm1*-shRNA 3 T3-L1 preadipocytes and NC 3 T3-L1 preadipocytes were induced to differentiate. On the 10th day of differentiation, total RNAs from 3 T3-L1 cells were extracted as described in the Materials and Methods. *Ucp2* mRNA relative to  $\beta$ -actin in the 3 T3-L1 adipocytes was examined by real-time PCR. \* $P<0.05$  in comparison with the NC adipocytes ( $n=6$ )

ROS levels. Figure 6 shows that the levels of *Ucp2* mRNA in the *Lyrm1* knockdown adipocytes were dramatically increased compared with NC adipocytes.

## Discussion

Mitochondria are intracellular organelles with a highly dynamic state that generate ATP through oxidative phosphorylation. The efficiency of ATP production reflects the integrity of mitochondrial function. In mitochondria, ATP production is coupled to an electron transport system, in which the pumping of protons from matrix into the intermembrane space generates an electrochemical gradient of protons that consists of a  $\Delta\Psi_m$  and pH gradient. The mitochondrial  $\Delta\Psi_m$  is fundamental for the conversion of ADP to ATP via ATP synthase (Brown 1992) and a sustained elevation of  $\Delta\Psi_m$  is known to elevate the production of ROS, a byproduct of the electron transport chain, due to the continuous generation of superoxide species within mitochondria. High concentrations of ROS due to the imbalance between ROS production and its removal can directly damage the mitochondrial proteins, DNA and lipids in membrane components, resulting in mitochondrial dysfunction (Fridlyand and Philipson 2006). A slight increase in mitochondrial ROS production would induce the deglutathionylation of UCP2. UCP2 belongs to a superfamily of mitochondrial transporters that uncouple ATP synthesis from electron transport and thereby their activities, which subsequently would decrease ROS production (Mailloux and Harper 2011). Earlier studies (Cao et al. 2010; Qiu et al. 2009) have demonstrated that LYRM1, a new candidate gene for obesity, was expressed at a higher level in obese subjects than in normal-weight controls, and the overexpression of *Lyrm1* in mouse adipocytes was shown to induce mitochondrial dysfunction characterized by abnormal mitochondrial morphology, lower ATP content and mitochondrial membrane potentials and increased ROS levels. The levels of insulin-stimulated glucose uptake were decreased.

Accumulated evidence has shown that mitochondrial dysfunction plays an important role in the pathogenesis of IR. A previous study (Cao et al. 2010) also showed that the overexpression of *Lyrm1* in adipocytes induced mitochondrial dysfunction. Therefore, we further investigated the effects of the *Lyrm1* knockdown on mitochondrial function in adipocytes. Our results showed that suppression of *Lyrm1* had no obvious effect on the morphology and number of mitochondria, as there was no obvious difference in both mtDNA copy number and the ultrastructure of mitochondria between *Lyrm1*-RNAi adipocytes and NC (negative control) adipocytes. Furthermore, increased ATP synthesis, elevated  $\Delta\Psi_m$ , decreased intracellular ROS production and increased levels of *Ucp2* mRNA were observed in *Lyrm1*

knockdown adipocytes. Those observations revealed that inhibition of *Lyrm1* expression affected mitochondrial function to some extent. The elevated production of ATP may represent partially improved mitochondrial function, which may have been induced by the increased  $\Delta\Psi_m$  instead of mitochondrial morphology and copy number.

The level of ROS in the *Lyrm1*-silenced adipocytes was significantly lower than in the NC adipocytes. Several possible reasons could exist for this phenomenon. Firstly, it may have resulted from the restored mitochondrial function. Mitochondria have several ROS detoxifying systems, which maintain the balance between ROS production in and removal from these organelles (Andreyev et al. 2005). Secondly, a slight increase in mitochondrial ROS production caused by the improved mitochondrial ATP synthesis would induce the deglutathionylation of Ucp2 and thereby their activities, which subsequently would decrease ROS production. In addition, LYRM1 contains a LYR-motif, which is present in the N-terminal region in several protein sequences in different species. There are several kinds LYR-motif (LYRM) proteins in humans. Several studies (Cardol et al. 2004; Ghezzi et al. 2009; Wiedemann et al. 2006; Ye and Connor 2000) have suggested that the LYR-motif is a signature for proteins involved Fe-S metabolism. Whether LYRM1 is involved in Fe-S metabolism, electron transfer and influencing mitochondrial function, remains incompletely understood.

In summary, our results revealed that the *Lyrm1* knockdown improved mitochondrial function in mature adipocytes, with elevated  $\Delta\Psi_m$ , increased cellular ATP production and decreased ROS production. This gene may be a potential target for the treatment of obesity-related mitochondrial dysfunction. Further studies are needed to elucidate the underlying function of LYRM1 and its mechanisms of action *in vivo*.

**Acknowledgments** This work was supported by grants from the National Natural Science Foundation of China (grant numbers 30801256 and 81000348), and the Nanjing Municipal Foundation for Medical Science Development (ZKX09012).

## References

- Andreyev AY, Kushnareva YE, Starkov AA (2005) Mitochondrial metabolism of reactive oxygen species. *Biochemistry (Mosc)* 70:200–214
- Brocard JB, Rintoul GL, Reynolds IJ (2003) New perspectives on mitochondrial morphology in cell function. *Biol Cell* 95:239–242
- Brown GC (1992) Control of respiration and ATP synthesis in mammalian mitochondria and cells. *Biochem J* 284(Pt 1):1–13
- Cao XG, Kou CZ, Zhao YP, Gao CL, Zhu C, Zhang CM, Ji CB, Qin DN, Zhang M, Guo XR (2010) Overexpression of LYRM1 induces mitochondrial impairment in 3 T3-L1 adipocytes. *Mol Genet Metab* 101:395–399

Cardol P, Vanrobaeys F, Devreese B, Van Beeumen J, Matagne RF, Remacle C (2004) Higher plant-like subunit composition of mitochondrial complex I from *Chlamydomonas reinhardtii*: 31 conserved components among eukaryotes. *Biochim Biophys Acta* 1658:212–224

Chen C, Okayama H (1987) High-efficiency transformation of mammalian cells by plasmid DNA. *Mol Cell Biol* 7:2745–2752

Choo HJ, Kim JH, Kwon OB, Lee CS, Mun JY, Han SS, Yoon YS, Yoon G, Choi KM, Ko YG (2006) Mitochondria are impaired in the adipocytes of type 2 diabetic mice. *Diabetologia* 49:784–791

Dahlman I, Forsgren M, Sjogren A, Nordstrom EA, Kaaman M, Naslund E, Attersand A, Arner P (2006) Downregulation of electron transport chain genes in visceral adipose tissue in type 2 diabetes independent of obesity and possibly involving tumor necrosis factor-alpha. *Diabetes* 55:1792–1799

Ferrannini E, Balkau B, Coppack SW, Dekker JM, Mari A, Nolan J, Walker M, Natali A, Beck-Nielsen H (2007) Insulin resistance, insulin response, and obesity as indicators of metabolic risk. *J Clin Endocrinol Metab* 92:2885–2892

Fridlyand LE, Philipson LH (2006) Reactive species and early manifestation of insulin resistance in type 2 diabetes. *Diabetes Obes Metab* 8:136–145

Ghezzi D, Goffrini P, Uziel G, Horvath R, Klopstock T, Lochmuller H, D'Adamo P, Gasparini P, Strom TM, Prokisch H, Invernizzi F, Ferrero I, Zeviani M (2009) SDHAF1, encoding a LYR complex-II specific assembly factor, is mutated in SDH-defective infantile leukoencephalopathy. *Nat Genet* 41:654–656

Hammarstedt A, Jansson PA, Wesslau C, Yang X, Smith U (2003) Reduced expression of PGC-1 and insulin-signaling molecules in adipose tissue is associated with insulin resistance. *Biochem Biophys Res Commun* 301:578–582

Jeffery RW, Sherwood NE (2008) Is the obesity epidemic exaggerated? *No BMJ* 336:245

Kaaman M, Sparks LM, van Harmelen V, Smith SR, Sjolin E, Dahlman I, Arner P (2007) Strong association between mitochondrial DNA copy number and lipogenesis in human white adipose tissue. *Diabetologia* 50:2526–2533

Kahn CR (1978) Insulin resistance, insulin insensitivity, and insulin unresponsiveness: a necessary distinction. *Metabolism* 27:1893–1902

Kim JA, Wei Y, Sowers JR (2008) Role of mitochondrial dysfunction in insulin resistance. *Circ Res* 102:401–414

Kopelman PG (2000) Obesity as a medical problem. *Nature* 404:635–643

Lowell BB, Shulman GI (2005) Mitochondrial dysfunction and type 2 diabetes. *Science* 307:384–387

Maasen JA (2008) Mitochondria, body fat and type 2 diabetes: what is the connection? *Minerva Med* 99:241–251

Mailloux RJ, Harper ME (2011) Uncoupling proteins and the control of mitochondrial reactive oxygen species production. *Free Radic Biol Med*

Maxwell DP, Wang Y, McIntosh L (1999) The alternative oxidase lowers mitochondrial reactive oxygen production in plant cells. *Proc Natl Acad Sci U S A* 96:8271–8276

Niimi M, Tao L, Lin SH, Yin J, Wu X, Fukui H, Kambayashi J, Ye J, Sun B (2009) Involvement of an alternatively spliced mitochondrial oxodicarboxylate carrier in adipogenesis in 3 T3-L1 cells. *J Biomed Sci* 16:92

Qatanani M, Lazar MA (2007) Mechanisms of obesity-associated insulin resistance: many choices on the menu. *Genes Dev* 21:1443–1455

Qiu J, Gao CL, Zhang M, Chen RH, Chi X, Liu F, Zhang CM, Ji CB, Chen XH, Zhao YP, Li XN, Tong ML, Ni YH, Guo XR (2009) LYRM1, a novel gene promotes proliferation and inhibits apoptosis of preadipocytes. *Eur J Endocrinol* 160:177–184

Qiu J, Ni YH, Gong HX, Fei L, Pan XQ, Guo M, Chen RH, Guo XR (2007) Identification of differentially expressed genes in omental adipose tissues of obese patients by suppression subtractive hybridization. *Biochem Biophys Res Commun* 352:469–478

Reaven GM (1997) Banting Lecture 1988. Role of insulin resistance in human disease. 1988. *Nutrition* 13: 65, 64, 66

Robin ED, Wong R (1988) Mitochondrial DNA molecules and virtual number of mitochondria per cell in mammalian cells. *J Cell Physiol* 136:507–513

Spiegelman BM, Flier JS (2001) Obesity and the regulation of energy balance. *Cell* 104:531–543

Visscher TL, Seidell JC (2001) The public health impact of obesity. *Annu Rev Public Health* 22:355–375

Walley AJ, Asher JE, Froguel P (2009) The genetic contribution to non-syndromic human obesity. *Nat Rev Genet* 10:431–442

Wiedemann N, Urzica E, Guiard B, Muller H, Lohaus C, Meyer HE, Ryan MT, Meisinger C, Muhlenhoff U, Lill R, Pfanner N (2006) Essential role of Isd11 in mitochondrial iron-sulfur cluster synthesis on Isu scaffold proteins. *EMBO J* 25:184–195

Ye Z, Connor JR (2000) cDNA cloning by amplification of circularized first strand cDNAs reveals non-IRE-regulated iron-responsive mRNAs. *Biochem Biophys Res Commun* 275:223–227